RR-66-506, 1966 (unpublished).
[20]J. M. Hansteen and O. P. Mosebekk, in Ref. 10.
[21]D. C. McGrary and P. Richard, Phys. Rev. A 5, 1249 (1972).
[22]D. S. Urch, J. Phys. C 3, 1275 (1970).
[23]M. H. Reilly, J. Phys. Chem. Solids 30, 1041 (1970).
[24]E. P. Domashevskaya and Ya. A. Ugai, in *X-Ray Spectra and Chemical Binding*, edited by A. Meisel (Karl Marx University, Leipzig, 1966), p. 70.
[25]W. Nefedow, Phys. Status Solidi 2, 904 (1962).

PHYSICAL REVIEW A VOLUME 6, NUMBER 6 DECEMBER 1972

$6\,^3P_1$-$6\,^3P_0$ Excitation Transfer in Mercury, Induced in Collisions with N_2 Molecules*

J. Pitre,† K. Hammond, and L. Krause
Department of Physics, University of Windsor, Windsor, Ontario, Canada
(Received 19 June 1972)

The cross section for the transition $6\,^3P_0 \rightarrow 6\,^3P_1$ in mercury, induced in collisions with N_2 molecules, has been determined by the method of delayed coincidences. The Hg $^3P_1$ state was excited by pulses of 2537-Å Hg resonance radiation and the decay of the long-lived 2537-Å afterglow was studied in relation to N_2 pressure. The resulting cross section $Q_{12}(^3P_0 \rightarrow {}^3P_1) = 4.18 \times 10^{-4}$ Å^2 was found to be in good agreement with the prediction of the principle of detailed balancing when compared with the cross section $Q_{21}(^3P_1 \rightarrow {}^3P_0)$. It was also found that, within the sensitivity of the method, collisions with N_2 molecules do not quench $^3P_1$ or $^3P_0$ Hg atoms to the ground state.

I. INTRODUCTION

The quenching of the $6\,^3P_1$ state of mercury by collisions with nitrogen and other molecules has been studied extensively, but it is only recently that agreement was reached between values of quenching cross sections obtained in different laboratories.[1,2] The available cross sections tend to encompass the total collisional deexcitation of the $6\,^3P_1$ state, which may proceed by way of two channels: transition to the metastable state ($^3P_1 \rightarrow {}^3P_0$) and to the ground state ($^3P_1 \rightarrow {}^1S_0$). Horiguchi and Tsuchiya[3] have recently reported separate cross sections for these two processes but the sum of the cross sections disagreed with the total values determined elsewhere,[1,2] in some cases by a factor higher than two. Samson[4] reported the only attempt to obtain the cross section for the process $^3P_0 \rightarrow {}^3P_1$ but his experimental results had to be subjected to large corrections for radiation trapping. A comprehensive investigation of the production of $^3P_0$ Hg atoms by collisions between the $^3P_1$ atoms and N_2 molecules, and the subsequent depopulation of the metastable state by collisions with N_2 molecules, ground-state Hg atoms and vessel walls, as well as by absorption of Hg radiation, was carried out by Bigeon,[5] who concluded upon the relative magnitudes of the various effects but obtained no corresponding cross sections.

In the present investigation, the $6\,^3P_0 \rightarrow 6\,^3P_1$ transition induced in collisions between $6\,^3P_0$ mercury atoms and N_2 molecules was studied by the method of delayed coincidences in the long-lived afterglow from an Hg-N_2 mixture irradiated with pulses of 2537-Å mercury resonance radiation. The method has the advantage that complications arising from pressure broadening and from absorption of other mercury radiation are effectively absent. With N_2 pressures appropriately chosen, the migration to the walls of the $^3P_0$ metastable atoms could also be impeded. Finally, the Hg vapor pressure employed (5×10^{-6} torr) was over 300 times lower than in previous experiments of other investigators and was confined to a region where the effects due to the imprisonment of mercury resonance radiation and to collisional deactivation of $^3P_0$ atoms by ground-state atoms were insignificant.

II. THEORETICAL

Figure 1 shows a scheme of the energy levels in mercury that are involved in the various processes of excitation and decay. The states $^1S_0$, $^3P_0$, and $^3P_1$ are denoted as levels 0, 1, and 2, respectively, and the transitions between them are indicated by arrows. Solid arrows correspond to collisional transitions and broken arrows to spontaneous radiative transitions. It is assumed that these are the only processes that cause the depopulation of any state. The transition rates are denoted by the symbols Γ, singly subscribed for radiative transitions and doubly for collisional transitions. The transition rates Γ_1 and Γ_2 are the reciprocal lifetimes of the appropriate states and, in the absence of radiation trapping, are constant, but the collisional transition rates de-

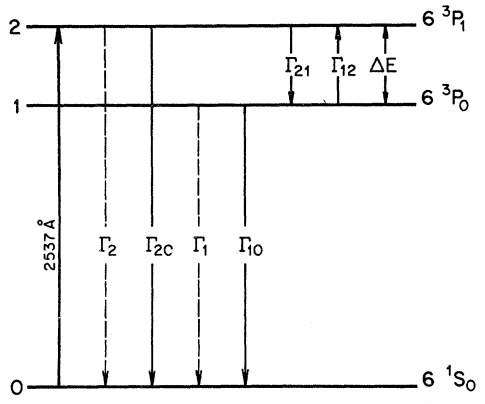

FIG. 1. Term diagram for Hg, showing levels and processes involved in the radiative and collisional transitions. The $^3P_1$-$^3P_0$ energy separation $\Delta E = 1767$ cm^{-1}.

pend on the pressure of the buffer gas (nitrogen).

The rates of change of the populations n_1 and n_2 of the states $^3P_0$ and $^3P_1$ may be represented as follows:

$$\dot{n}_1 = -(\Gamma_1 + \Gamma_{12} + \Gamma_{10})n_1 + \Gamma_{21} n_2 \quad , \tag{1}$$

$$\dot{n}_2 = -(\Gamma_2 + \Gamma_{21} + \Gamma_{20})n_2 + \Gamma_{12} n_1 \quad , \tag{2}$$

where, for example, Γ_{12} represents the frequency of collisions per Hg $6\,^3P_1$ atom, leading to the $^3P_0 \rightarrow {}^3P_1$ transition. The differentiation of Eq. (1) and substitution of n_1 and $\dot{n}_1$ into Eq. (2) result in a single second-order differential equation containing one variable:

$$\ddot{n}_2 + (\Gamma_1 + \Gamma_2 + \Gamma_{12} + \Gamma_{21} + \Gamma_{10} + \Gamma_{20})\dot{n}_2 + [(\Gamma_1 + \Gamma_{12} + \Gamma_{10})(\Gamma_2 + \Gamma_{21} + \Gamma_{20}) - \Gamma_{12}\Gamma_{21}]n_2 = 0. \tag{3}$$

Equation (3) has the form

$$\ddot{n}_2 + a\dot{n}_2 + bn_2 = 0 \tag{4}$$

and has a general solution of the form

$$n_2 = A\, e^{-\Gamma_A t} + B\, e^{-\Gamma_B t} \quad , \tag{5}$$

where

$$\Gamma_{A,B} = \tfrac{1}{2} a \pm (\tfrac{1}{4} a^2 - b)^{1/2} \quad . \tag{6}$$

In particular, without making any assumptions as to the magnitudes of the decay rates, we find

$$\Gamma_A = \frac{\Gamma_2 + \Gamma_{21} + \Gamma_{20} + (\Gamma_{12}\Gamma_{21})}{\Gamma_2 + \Gamma_{21} + \Gamma_{20} - \Gamma_1 - \Gamma_{12} - \Gamma_{10}} \quad , \tag{7}$$

$$\Gamma_B = \frac{\Gamma_1 + \Gamma_{12} + \Gamma_{10} - (\Gamma_{12}\Gamma_{21})}{\Gamma_2 + \Gamma_{21} + \Gamma_{20} - \Gamma_1 - \Gamma_{12} - \Gamma_{10}} \quad . \tag{8}$$

If the initial population of an excited state takes place by the absorption of a pulse of 2537-Å radiation which raises $^1S_0$ atoms to the $^3P_1$ state, and if one observes the emission of 2537-Å fluorescence from an Hg-N_2 mixture after the termination of the pulse, the fluorescence will decay in accordance with Eq. (5) and will exhibit two time-dependent components.

Short-Lived Component Γ_A

Equation (7) may be simplified by eliminating the fourth term on the right-hand side, as the result of the following considerations, which are valid at the nitrogen densities and relative velocities prevailing in this experiment: $\Gamma_1 \ll \Gamma_{21}$, since the lifetime of the $^3P_0$ state is of the order of 2s[5]; $\Gamma_{10}, \Gamma_{20} \ll \Gamma_{21}$, as shown by Horiguchi and Tsuchiya[3]; $\Gamma_{12} \ll \Gamma_{21}$ as shown by Samson[4] and also because $\Delta E \simeq 8kT$; $\Gamma_2 \simeq {}_{21}$ at reasonable N_2 pressures. At 72 torr of N_2, $\Gamma_2 = \Gamma_{21} + \Gamma_{20}$.[1] Equation (7) thus reduces to[6]

$$\Gamma_A = \Gamma_2 + \Gamma_{21} + \Gamma_{20} \quad . \tag{9}$$

Γ_A has been determined previously and was shown to have a minimal value corresponding to the "natural" lifetime of the $^3P_1$ state (117ns) in pure Hg vapor at low density and to increase linearly with N_2 pressure.[1]

Long-Lived Component Γ_B

Because $\Gamma_1 \ll \Gamma_{12}$ and $\Gamma_{10}, \Gamma_{12} \ll \Gamma_{21}$, Eq. (8) may be simplified to

$$\Gamma_B = \Gamma_{10} + \Gamma_{12} - \Gamma_{12}\Gamma_{21}/(\Gamma_2 + \Gamma_{21} + \Gamma_{20}) \tag{10}$$

$$= \Gamma_{10} + \Gamma_{12}(\Gamma_2 + \Gamma_{20})/(\Gamma_2 + \Gamma_{21} + \Gamma_{20}) \quad . \tag{11}$$

Γ_2 has been determined previously[7] as has the sum $\Gamma_{21} + \Gamma_{20}$, which may be obtained from the total-quenching cross section $Q = 0.72$ Å^2 and from the relation

$$\Gamma_{21} + \Gamma_{20} = N v_r Q \quad , \tag{12}$$

which defines the cross section in analogy with the gas-kinetic cross section (N is the density of the N_2 molecules and v_r is the average relative speed of the colliding partners). This information, when substituted in Eq. (11), yields the following expression for Γ_B:

$$\Gamma_B = \Gamma_{10} + [72\Gamma_{12}/(P + 72)](1 + 1.17 \times 10^{-7}\Gamma_{20}) \quad . \tag{13}$$

Equation (13) describes the curve obtained on plotting the measured decay constant of the 2537-Å long-lived afterglow in relation to the pressure P of N_2 (in torr), the precise shape of the curve depending on the magnitudes of Γ_{10}, Γ_{20}, and Γ_{12}.

III. EXPERIMENTAL

A schematic diagram of the apparatus is shown in Fig. 2. Light emitted from a mercury electrode-

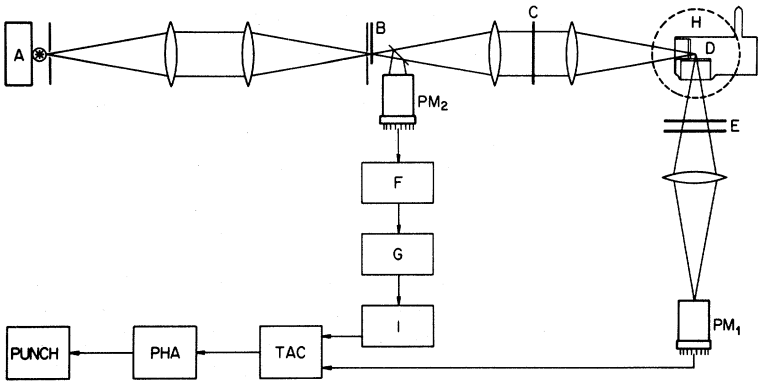

FIG. 2. Schematic diagram of the apparatus used in the experiment. A, lamp; B, chopper; C, color filter; D, fluorescence cell in oven; E, interference filters; PM_1, 56 TUVP photomultiplier; PM_2, auxiliary photomultiplier; F, amplifier; G, delay line; H, Helmholtz coils; I, pulse shaper; TAC, time-to-amplitude converter; PHA, pulse-height analyzer; PUNCH, paper-tape punch.

less discharge was chopped, passed through a filter to render it monochromatic, and brought to a focus in the fluorescence cell containing a Hg-N_2 mixture at a controlled temperature. The fluorescent light pulses emitted at right angles to the direction of excitation were passed through two Corion interference filters in tandem which had a bandwidth of 150 Å centered on 2537 Å, and were detected with a Philips 56 TUVP photomultiplier cooled with liquid nitrogen. The delays between the exciting and fluorescent light pulses were measured by reflecting a small part of the exciting light on to the photocathode of an auxiliary photomultiplier whose output pulses were applied to the "start" terminal of a time-to-amplitude converter to whose "stop" terminal were directed the pulses from the 56 TUVP photomultiplier. The resulting decay spectrum was accumulated in a 200-channel pulse-height analyzer and was finally transferred to punched paper tape.

The mercury discharge lamp consisted of a vertical quartz tube placed in a coil which formed part of a tank circuit of a 150-MHz oscillator. The lower end of the tube contained a drop of mercury and was maintained at a constant temperature of 48 °C by water circulating from a thermostatic bath. In this way it was possible to obtain the maximal intensity of the exciting light and to ensure excellent stability over many hours of operation. The light from the lamp passed through a slit 15 mm long and 1 mm wide and was brought to a focus at a similar slit immediately preceding a P.A.R. model 222 variable speed chopper equipped with a special wheel containing four 2-cm-wide tapered slits. The light pulses produced at 75 repetitions per second were rectangular, with rise and fall times of about 25-μsec, 500-μsec length, and had a repetition rate of 300/sec. The Corning CS7-54 filter was included in the light beam to prevent the mercury 6^3P_0 metastable atoms from being excited to higher states and to ensure the production of the highest possible density of metastable atoms at the end of each exciting light pulse.

The exciting light was brought to a focus in the rectangular corner between the entrance and observation windows of the fluorescence cell so that the paths of the incident and fluorescent light were restricted to about 2 mm, thus reducing the possibility of radiation trapping. The earth's magnetic field at the cell was canceled by means of a set of Helmholtz coils in order to eliminate modulation of the decay, which would otherwise take place during the experiments with pure Hg vapor.[8] The cell was fitted with a side arm which contained a drop of liquid mercury and which was maintained at a temperature of − 32 °C. In this way a constant mercury vapor pressure of 5×10^{-6} torr was maintained in the cell which was kept at 23 °C (corresponding to $v_r = 505$ m/sec) throughout the experiments. The cell and the vacuum and gas-filling system to which it was connected were carefully baked out under vacuum for prolonged periods of time. The pressure of nitrogen (Matheson, research grade) that could be admitted in controlled quantities was measured with a trapped C.V.C. type GM-100A McLeod gauge or with a trapped manometer.

Considerable attention was devoted to ensuring that the delay-time measurements were accurate and reliable. The voltage pulses from the reference photomultiplier were amplified and delayed until the end of each exciting pulse, and were appropriately shaped before reaching the Ortec 457S time-to-amplitude converter, which had a linearity better than 1%. The multichannel analyzer was calibrated with an Ad-Yu model 802E delay line with an accuracy better than 2%. Because of some attenuation and decrease in rise time of pulses in a passive delay line as longer delays of up to 2 msec are reached, it was necessary to amplify and shape pulses that had passed through the delay line in order to achieve the specified accuracy of the time-to-amplitude converter. The linearity of the TAC-multichannel analyzer system, as well as the accuracy of the

time delay, was verified by the fact that a plot of channel number against delay time was linear over the entire range of 200 channels to within one channel and remained so for several days at a time.

The experimental data accumulated in the multichannel analyzer were obtained on punched-paper tape and were subjected to analysis for the exponential decay on an IBM 360-50 computer, using a modified FRANTIC program.[9] One of the modifications consisted of a small correction for discrimination against the detection of longer-lived excited atoms.[10] This correction amounted to only a few percent, with counting rates of about 30/sec, equivalent to about one photon detected for every ten exciting pulses.

IV. RESULTS AND DISCUSSION

Pulse-height spectra resulting from the decay of the 2537-Å long-lived afterglow were obtained at various nitrogen pressures and the decay constants Γ_B extracted from these data were plotted against N_2 pressure as shown in Fig. 3. Each decay spectrum required about 1 h to accumulate and each point in Fig. 3 represents the average of two such spectra. The largest divergence between any two values of Γ_B obtained at the same pressure did not exceed 4.2%, but the average divergence between such pairs of Γ_B obtained at pressures above 30 torr (which were used exclusively in the final calculation) amounted to 1.2%.

At pressures above 30 torr, there are only small effects arising from the diffusion of the $^3P_0$ metastable atoms to the walls of the cell. The experimental data in this range could only be fitted to Eq. (13) by assuming $Q_{10}=Q_{20}=0$, and yielded the preliminary value $Q_{12}=4.2\times10^{-4}$ Å^2.

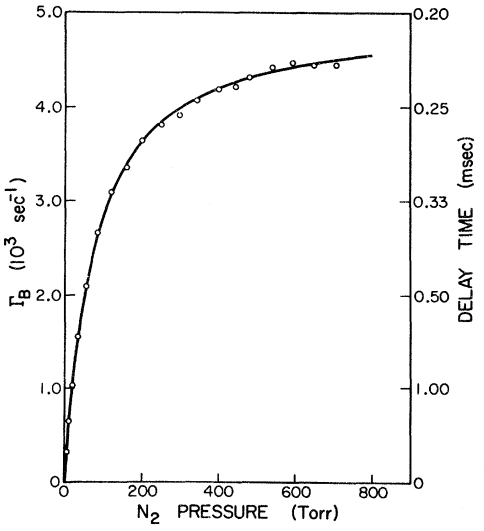

FIG. 3. Variation of the decay constant Γ_B with N_2 pressure. Low-pressure values have been corrected for diffusion to the walls.

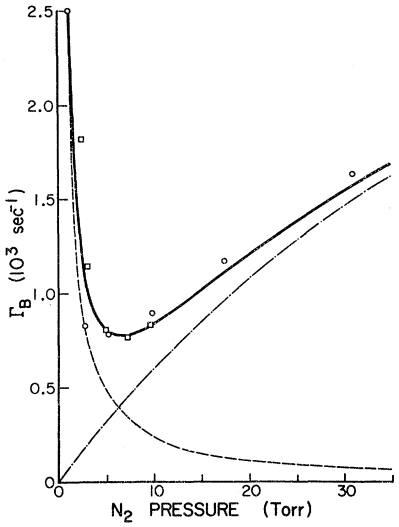

FIG. 4. Variation of Γ_B with N_2 pressure in the low-pressure region. The points ⊙ and ⊡ represent different experimental runs and have not been corrected for diffusion to the walls. The dashed-dotted line represents a plot of Eq. (13); the dashed line represents $\Gamma=k/P$; and the solid line represents the result of adding the two other curves.

It was thought worthwhile to consider in some detail the influence of the diffusion of the $^3P_0$ metastable atoms on the experimental results at low pressures. Figure 4 shows the values of Γ_B obtained at low pressures, some of which were lost in Fig. 3, as well as some additional results obtained in another experiment. The figure also includes a plot of Eq. (13) with $Q_{10}=Q_{20}=0$ and $Q_{12}=4.2\times10^{-4}$ Å^2, and a plot of the function $\Gamma=k/P$ representing the effects of the diffusion at a pressure P of N_2 on the decay constant. The constant k was chosen to give the best fit of the result of the addition of these two functions to the experimental data. In plotting the diffusion curve, we assumed the value 49 Å^2 for the diffusion cross section,[4] as well as a parallel-plate geometry, even though the latter is only a very rough approximation to the conditions in the fluorescence cell. The fitting procedure yielded a diffusion length of about 7 mm, which is reasonable if it is considered that, even though the exciting light beam is focused 2 mm from the observation window, $^3P_0$ atoms may move up to 2 cm away from the window (before striking the cell wall) and still remain in the field of view. It was concluded on the basis of these considerations that at pressures above 30 torr, corrections to the experimental data for diffusion effects should not exceed 5%.

The effects on the experimental results of possible long-lived fluorescence of the quartz of which the cell was constructed, were also investigated. Such effects would exert the largest influence at low nitrogen pressures, where the true fluorescent signal is weakest. Even though two 2537-Å interference filters were inserted in the fluorescent light path to eliminate the well-known fluorescent band of quartz that falls in the vicinity of 4200 Å, at the lowest nitrogen pressures it was still possible to discern an effect of quartz fluorescence with a decay time of 107 μsec. This made necessary further corrections to the measured values of Γ_B, typically amounting to 1% at 31 torr and becoming insignificant at higher pressures. Additional small corrections were made for continuous stray light and noise in the photomultiplier but the signal-to-noise ratio was usually 100:1 or better.

With the inclusion of these various corrections, the experimental data, obtained at nitrogen pressures above 30 torr, yielded the final value $Q_{12} = 4.18\times10^{-4}$ Å^2. The uncertainty in this result is determined not only by the statistics of a single experiment, but also by the reproducibility of the curves shown in Figs. 3 and 4 with different samples of N_2, since quenching to the ground state by impurities would drastically influence the shapes of the curves. The Matheson research grade nitrogen that was used in the experiments is specified to include less than one ppm of all potential quenching contaminants whose effect would be to increase the effective value of Γ_{10} in Eq. (13). For example, the presence of a few parts in 10^7 of H_2, which has a quenching cross section[3] $Q_{10} = 6.6$ Å^2, would be detectable in the analysis of the results as a linear increase of Γ_B with pressure. In order to reduce similar quenching effects of any impurities remaining on the walls of the cell, all experimental runs were begun at high N_2 pressure which was then gradually reduced in the course of the run. In addition to the data shown in Figs. 3 and 4, we carried out 20 additional determinations at various N_2 pressures to test for possible accumulation of impurities in the cell with time, of which there was no evidence. The consideration of all these possible sources of error, as well as of error inherent in the pressure and time calibration, leads to a total limit of error of ± 3% in the cross section Q_{12}.

Upper limits may also be placed on the quenching cross sections Q_{10} and Q_{20}. Assuming that a linear contribution to Γ_B of 3×10^2 sec^{-1} at 700 torr might be detectable in the analysis of the data leads to the maximal values $Q_{10} \leq 2\times10^{-6}$ Å^2 and $Q_{20} \leq 4\times10^{-3}$ Å^2, which are considerably lower than values proposed by other authors that are summarized in Table I. It thus appears that the previously obtained cross section for the total quenching of Hg $6\,^3P_1$ atoms[1] (0.72 Å^2) corresponds to Q_{21}. This conclusion agrees with the results obtained by Callear and Hedges,[11] who found that nitrogen quenches Hg $6\,^3P_1$ atoms to the $^3P_0$ state to the extent of at least 90%. The ratio of the measured cross sections $Q_{12}/Q_{21} = 5.6\times10^{-4}$ agrees satisfactorily with the value 5.8×10^{-4} predicted from the principle of detailed balancing. These results and especially the cross section Q_{12} are in remarkably good agreement with the values obtained by Samson many years ago.[4] Samson's value $Q_{12} = 0.21$ Å^2 must, however, be multiplied by the factor $(1+\Delta E/kT)e^{-\Delta E/kT}$ to permit a direct comparison [see Eq. (27) of Ref. 4].

TABLE I. Cross sections for collisions of $^3P_1$ and $^3P_0$ Hg atoms with N_2 molecules.

Source	Collision cross sections (Å^2) $Q_{12}(^3P_0 \rightarrow {}^3P_1)$	$Q_{21}(^3P_1 \rightarrow {}^3P_0)$	$Q_{10}(^3P_0 \rightarrow {}^1S_0)$	$Q_{20}(^3P_1 \rightarrow {}^1S_0)$
This investigation	4.18×10^{-4}	0.72[a]	$\leq 2\times10^{-6}$	$\leq 4\times10^{-3}$
Ref. 4	3.8×10^{-4}[b]	0.97	$\leq 6.3\times10^{-6}$	$\leq 6.9\times10^{-2}$
Ref. 3	...	1.1	$\leq 2.5\times10^{-5}$	$\leq 9.4\times10^{-2}$

[a]Value taken from Ref. 1.

[b]Represents Samson's (Ref. 4) quoted value 0.21 Å^2 multiplied by the factor $(1+\Delta E/kT)e^{-\Delta E/kT}$.

It is likely that the $^3P_1 \rightleftharpoons {}^3P_0$ excitation-transfer processes take place according to the mechanism

$$\mathrm{Hg}(^3P_1) + \mathrm{N}_2(v=0) \rightleftharpoons \mathrm{Hg}(^3P_0) + \mathrm{N}_2(v=1), \qquad (14)$$

since the $^3P_1$-$^3P_0$ energy separation equals 1767 cm^{-1} and the energy of the vibrational transition in nitrogen is 2330 cm^{-1}. A mechanism involving N_2 in its ground vibrational state on both sides of Eq. (14) seems considerably less likely.

The interaction between Hg $^3P_1$ atoms and N_2 molecules exhibits the very specific property of quenching exclusively to the $^3P_0$ metastable state (within the limits of the sensitivity of the experiment). In contrast, CO quenches both the $^3P_1$ and $^3P_0$ states to the ground state[12] and an attempt to observe long-lived-Hg 2537-Å afterglow in its presence was not successful.

*Research supported by the Aeronautical Systems Division of Wright-Patterson Air Force Base, through the U. S. Department of the Air Force, under Contract No. F. 33615-68-C-1511, and by the National Research Council of Canada.

†Present address: Department of Physics, University of Toronto, Toronto, Ontario, Canada.

[1]J. S. Deech, J. Pitre, and L. Krause, Can. J. Phys. 49, 1976 (1971).

[2]J. P. Barrat, D. Casalta, J. L. Cojan, and J. Hamel, J. Phys. Radium 27, 608 (1966).

[3]H. Horiguchi and S. Tsuchiya, Bull. Chem. Soc.

Japan 44, 1213 (1971).
[4]E. Samson, Phys. Rev. 40, 940 (1932).
[5]M. C. Bigeon, J. Phys. Radium 28, 157 (1967).
[6]The quantities Γ_A, Γ_2, and $(\Gamma_{21}+\Gamma_{20})$ are equivalent to Γ_0, Γ, and Z_Q, respectively, of Ref. 1.
[7]J. S. Deech and W. E. Baylis, Can. J. Phys. 49, 90 (1971).
[8]A. Corney and G. W. Series, Proc. Phys. Soc. (London) 83, 207 (1964).
[9]P. C. Rogers, FRANTIC, program for analysis of exponential growth and decay curves, M.I.T. Laboratory of Nuclear Sciences Technical Report No. 76, 1962 (unpublished).
[10]P. B. Coates, J. Phys. E 1, 878 (1968).
[11]A. B. Callear and R. E. M. Hedges, Trans. Faraday Soc. 66, 605 (1970).
[12]M. D. Scheer and J. Fine, J. Chem. Phys. 36, 1264 (1962).

PHYSICAL REVIEW A VOLUME 6, NUMBER 6 DECEMBER 1972

Electron-Impact Excitation Cross Sections for Atomic Oxygen: ^3P-$3s\,^3S^0$†*

Steven P. Rountree and Ronald J. W. Henry
Department of Physics and Astronomy, Louisiana State University, Baton Rouge, Louisiana 70803
(Received 27 June 1972)

Electron-impact excitation cross sections for O I (^3P-$3s\,^3S^0$) are calculated in unitarized Born, nonexchange, and close-coupling approximations. The close-coupling cross sections have the same energy dependence as measurements by Stone and Zipf but are lower in magnitude by a factor of 4. Two autodetaching levels of $O^-[2p^3(^4S^0)3s3p\ ^{2,4}P]$ are found at 9.67 and 9.94 eV. The doublet state is tentatively identified as a state found experimentally by Edwards at 9.52 eV.

The electron-impact excitation cross section for O I (^3P-$3s\,^3S^0$) is of interest in the atmospheric physics of Earth[1] and Mars.[2] Fast photoelectrons, produced in the upper atmosphere of the Earth by the absorption of solar ultraviolet radiation by the neutral constituents, lose energy in collision processes. The excitation of the neutral particles produces a substantial component of the dayglow luminosity of the upper atmosphere and the resonance triplet of atomic oxygen

$$O(2p^3 3s\,^3S^0) \rightarrow O(2p^4\,^3P) + h\nu$$

is one of the prominent features.

Recently, an experimental determination of this excitation cross section has been made by Stone and Zipf.[3] The only previous theoretical calculation[4] for this process is based on an impact-parameter method. Stauffer and McDowell's results probably give only an order-of-magnitude estimate in the low-energy region. They predict a broad maximum at 50 eV, which contrasts with Stone and Zipf's measurements of a broad maximum at 20 eV. At high energies, this impact-parameter method gives cross sections of about a factor of 3 higher than experiment. Since these measurements include cascade effects as well as the direct excitation process, they represent an upper limit to the cross section.

We calculate the excitation cross section in the unitarized Born, the nonexchange, and two-state close-coupling approximations. The general theory of the close-coupling approximation for complex atoms has been given by Smith and Morgan.[5]

We expand the total wave function for the system in a two-state close-coupling expansion in terms of the ground $1s^2 2s^2 2p^4(^3P)$ state and the excited $1s^2 2s^2 2p^3(^4S)3s(^3S^0)$ state of the oxygen atom. A partial-wave expansion is made for the wave function for the incident electron. The resulting close-coupling equations for the radial motion of the incident electron are solved numerically by using the procedures outlined by Smith, Henry, and Burke.[6]

Since we are considering an optically allowed excitation process, many partial waves contribute to the total inelastic cross section. For large values of the orbital angular momentum of the electron, we calculate the partial cross section in the unitarized Born approximation.[7] This is a valid procedure since, in the important interaction region, the centrifugal barrier term dominates the direct- and exchange-interaction potentials, and solutions of the radial equations are just spherical Bessel functions.

In the collision problem, the wave functions of the target system are assumed to be known. Kelly[8] has presented self-consistent-field (SCF) functions in analytical form for oxygen in the configuration $1s^2 2s^2 2p^3(^4S^0)3s\,^3S^0$. Kelly's 3s orbital will be referred to by 3sK. An alternative representation of the 3s orbital has been generated